Ocean lidar measurements of beam attenuation and a roadmap to accurate phytoplankton biomass estimates

Yongxiang Hu, Mike Behrenfeld, Chris Hostetler, Jacques Pelon, Charles Trepte, Johnathan Hair, Wayne Slade, Ivona Cetinic, Mark Vaughan, Xiaomei Lu, et al.

EPJ Web of Conferences **119**, 22003 (2016) DOI: 10.1051/epjconf/201611922003
ILRC 27

OCEAN LIDAR MEASUREMENTS OF BEAM ATTENUATION AND A ROADMAP TO ACCURATE PHYTOPLANKTON BIOMASS ESTIMATES

Yongxiang Hu[1]*, Mike Behrenfeld[2], Chris Hostetler[1], Jacques Pelon[3], Charles Trepte[1], John Hair[1], Wayne Slade[4], Ivona Cetinic[5], Mark Vaughan[1], Xiaomei Lu[1], Pengwang Zhai[6], Carl Weimer[7], David Winker[1], Carolus C. Verhappen[1], Carolyn Butler[1], Zhaoyan Liu[1], Bill Hunt[1], Ali Omar[1], Sharon Rodier[1], Anne Lifermann[2], Damien Josset[8], Weilin Hou[8], David MacDonnell[1], Ray Rhew[1]

*[1]NASA Langley Research Center, Hampton, VA 23681, USA, *Email: Yongxiang.hu-1@nasa.gov*

[2]Oregon State University, Corvalis, OR, USA; [3]Centre National d'Etudes Spatiales, France

[4]Sequoia Sci. Inc., USA; [5]University of Maine, Walpole, ME 04573; [6]UMBC, MD, USA;

[7]Ball Aerospace Corp., CO, USA; [8]NRL Stennis, MS, USA

ABSTRACT

Beam attenuation coefficient, *c*, provides an important optical index of plankton standing stocks, such as phytoplankton biomass and total particulate carbon concentration. Unfortunately, *c* has proven difficult to quantify through remote sensing. Here, we introduce an innovative approach for estimating *c* using lidar depolarization measurements and diffuse attenuation coefficients from ocean color products or lidar measurements of Brillouin scattering. The new approach is based on a theoretical formula established from Monte Carlo simulations that links the depolarization ratio of sea water to the ratio of diffuse attenuation K_d and beam attenuation C (i.e., a multiple scattering factor).

On July 17, 2014, the CALIPSO satellite was tilted 30° off-nadir for one nighttime orbit in order to minimize ocean surface backscatter and demonstrate the lidar ocean subsurface measurement concept from space. Depolarization ratios of ocean subsurface backscatter are measured accurately. Beam attenuation coefficients computed from the depolarization ratio measurements compare well with empirical estimates from ocean color measurements. We further verify the beam attenuation coefficient retrievals using aircraft-based high spectral resolution lidar (HSRL) data that are collocated with in-water optical measurements.

1. INTRODUCTION OF THE CONCEPT

Though originally designed for retrieving spatial and optical properties of clouds and aerosols, new applications of CALIOP measurements suggest that space-based lidars can provide physical properties of ocean surface [1] and subsurface [2][3]. Lidars can be used for retrievals of particulate backscattering, diffuse attenuation coefficients, the size spectrum and vertical distribution of ocean particles. These retrievals complement products derived from passive ocean color sensors and can contribute to reduced uncertainties in global ocean plankton stocks, primary productivity, and carbon export estimates. Here, we introduce an innovative approach for retrieving the beam attenuation coefficient from the subsurface depolarization ratio measured with space-based and/or aircraft-based lidars.

The beam attenuation coefficient, *c*, has proven an elusive ocean property to retrieve from remote sensing measurements [4]. One approach has been to estimate *C* from chlorophyll concentration [5], but this approach can suffer from chlorophyll (1) being influenced by physiological processes (i.e., intracellular changes in pigmentation in response to light and nutrient conditions) [6] and (2) not providing a robust index of the non-phytoplankton particle populations. Due to the highly forward peaked scattering phase function in water (with asymmetry factor around 0.95), we can only measure the effective attenuation coefficient (K_d), which is linked to *C* through the so-called multiple scattering factor, η ($\eta=K_d/c$). Accurately quantifying the magnitude and effects of multiple scattering is the primary obstacle in obtaining reliable measurements of *c* [4].

Multiple scattering can cause depolarization [7]. Thus for non-absorbing media with spherical particles, η can be estimated accurately from lidar depolarization measurements [8][9][10]. Monte Carlo simulations of ocean lidar backscatter suggest that a similar relationship between multiple scattering factor and depolarization ratio (δ) exists for absorbing media as well, i.e.,

$$\eta = \left(\frac{\varpi^2 - \delta}{\varpi^2 + \delta} \right)^2 , \tag{1}$$

where ϖ is the ratio of scattering and extinction coefficients for the water and its constituents. For open ocean at 532 nm, $\varpi \approx 1-\eta$ [11] and thus,

$$1 - \varpi \approx \left(\frac{\varpi^2 - \delta}{\varpi^2 + \delta} \right)^2 . \tag{2}$$

Solving Eq. 2, ω and η (=1-ω) can be derived from depolarization, δ (red line in Fig. 1),

$$K_d / c = 1 - \varpi = e^{-f(\delta)} . \tag{3}$$

When δ>0.002, $f(\delta) \approx 0.222+19.46\delta-188.39\delta^2+1288.1\delta^3-3974.9\delta^4+4684.2\delta^5$ and

$$c = K_d e^{f(\delta)} . \tag{4}$$

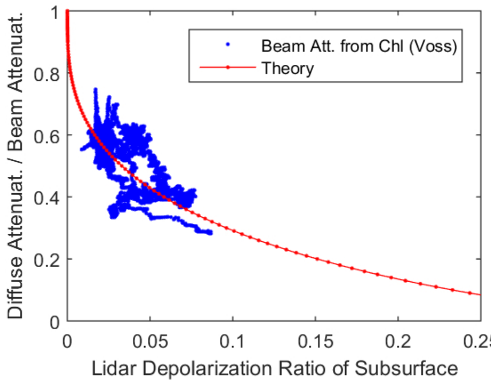

Figure 1. Solution of Equation (2) (red line). Comparison with collocated MODIS *c* (Voss, 1992).

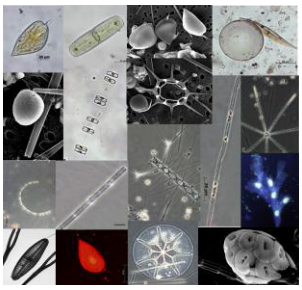

Figure 2. Microphotographs of phytoplankton cells demonstrating high diversity in morphological structures.

Eq. 2 is valid for sea waters with relatively small depolarization in backscatter direction. Depolarization ratios are near zero for backscatter by density fluctuation (Brillouin scattering) and for small soft particles with small relative refractice index. It is also likely valid for sea waters that may include some larger, non-spherical particulates, since the contribution of larger particulate to backscatter is relatively small and its bulk scattering properties are determined primarily by the tiny structures within the particles (Fig. 2) that have single scattering properties similar to spherical particles.

2. CALIPSO 30° Tilt: DEMONSTRATING OCEAN LIDAR IN SPACE

CALIOP's vertical resolution at 532 nm is 30 m. At average open ocean surface wind speeds (~6 m/s), the attenuated backscatter (532 nm parallel channel) from the ocean surface is about 30 times stronger than the subsurface backscatter. This makes it difficult to estimate the depolarization ratio of light backscattered by the ocean subsurface and to show clear ocean subsurface signals from CALIOP measurements.

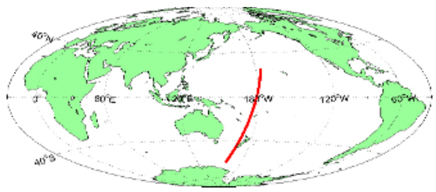

Figure 3. Orbit track when CALIPSO spacecraft is tilted 30° backward on July 17, 2014.

If the lidar is pointed 30^0 off-nadir, the ocean surface signal is reduced by more than two orders of magnitude [4], and CALIOP can then accurately measure ocean subsurface backscatter. The small surface contribution to 532 nm subsurfacebackscatter can be removed using 1064 nm measurements as its subsurface signals are near zero due to stronger absorption by water. Thus a 30° tilt of the CALIPSO satellite (and thus the CALIOP lidar) can help demonstrate our space-based ocean lidar concept.

CNES and NASA tilted the CALIPSO satellite 30^0 forward on July 17, 2014 (Fig. 3) in order to make accurate ocean subsurface backscatter measurements. During this special operation, CALIOP clearly detected ocean subsurface signals from both 532 nm parallel (upper panel, Fig. 4) and perpendicular (middle panel, Fig. 4) channels. Very little backscatter is seen in the 1064 nm channel (lower panel of Figure 4) near the ocean surface. It suggests that the ocean surface does not contribute to the subsurface signal in the 532 nm channels, because ocean surface backscatter at 532 nm is about 30% less than ocean surface backscatter at 1064 nm. Both the parallel and perpendicular components of 532nm backscatter are measured accurately by CALIOP at 30^0 off-nadir. The column integrated depolarization ratio of ocean subsurface backscatter can be accurately measured.

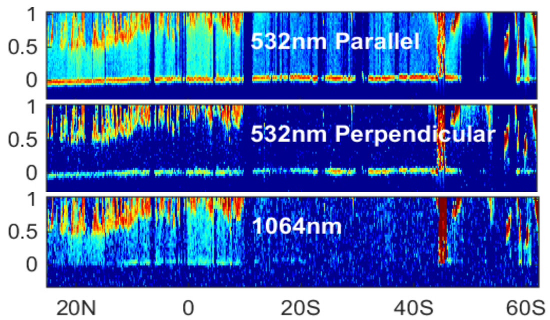

Figure 4. The lowest 1 km CALIOP backscatter profiles. Upper panel: 532 nm parallel; lower panel: 1064 nm total; middle panel: 532nm perpendicular.

3. COMPARISON OF BEAM C: CALIOP vs MODIS

Figure 5 shows beam c (red line) derived from CALIOP depolarization measurements (blue line) together with collocated MODIS diffuse attenuation coefficient estimates scaled to 532 nm (black line). Difference between CALIOP's *c* estimates and *c* based on MODIS chlorophyll measurements (green line) [7] are mostly within 30%.

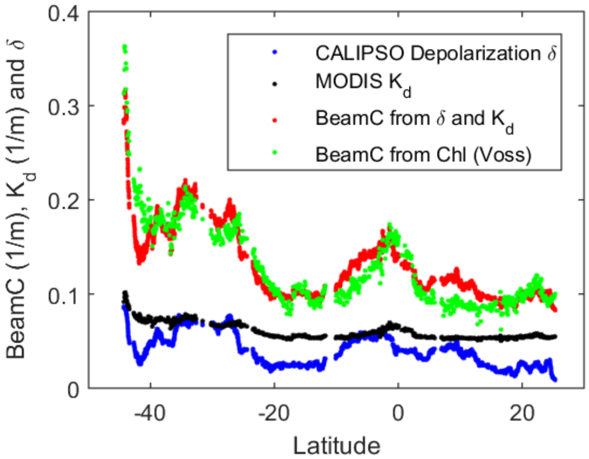

Figure 5. Beam attenuation coefficient comparisons between the lidar (red) method and the chlorophyll (green) method.

4. COMPARISONS BETWEEN AIRCRAFT LIDAR AND IN WATER MEASUREMENTS

During July 2014, NASA's Ship-Aircraft Bio-Optical Research project (SABOR) acquired both aircaft HSRL measurements [12] and in-water optical measurements along the track of an ocean-going research vessel [13]. Here we compare the beam attenuation coefficients derived from the lidar and the in-water measurements for the aircraft flight on July 26, where the flight track (red line in Figure 6) is close to the ship track (green).

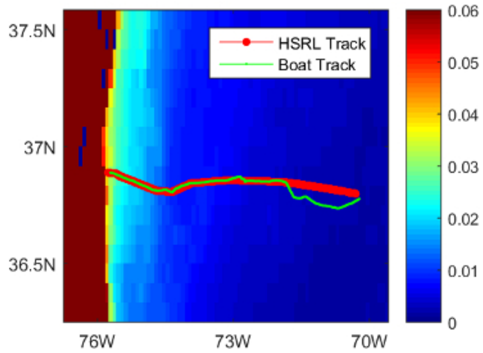

Figure 6. Aircraft track (red line) and track of the research vessel (green). The background is CDOM absorption coefficient (m^{-1}) estimated rom MODIS.

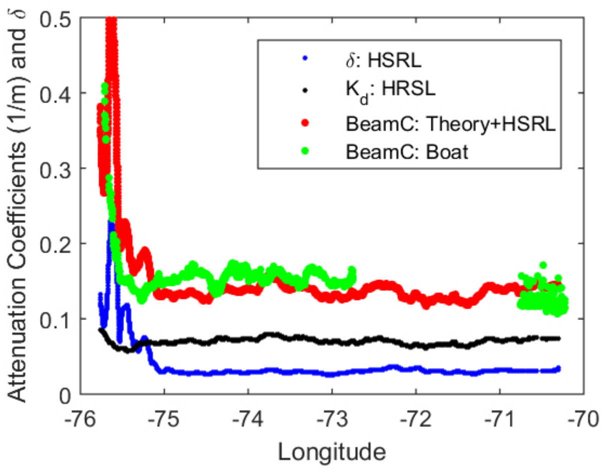

Figure 7. Beam attenuation coefficient comparisons between the HSRL lidar (red) and in water (green) measurements.

Because Brillouin backscatter is frequency shifted, HSRL can make separate measurements of particulate backscatter $\beta_P(z)$ and Brillouin scattering $\beta_B(z)$ profiles. HSRL provides accurate subsurface depolarization measurements (blue line in Figure 7), and can measure K_d directly from the vertical Brillouin backscatter profile as $K_d=-\Delta\log[\beta_B(z)]/\Delta z$. K_d can also be computed from the column integrated Brillouin signal, which is inversely proportional to diffuse attenuation (black line in Figure 7),

$$K_d = a\beta_m / \beta_B \quad , \qquad (5)$$

where β_m is the molecular backscatter signal of the air right above the ocean surface, and a is a constant related to instrument filter characteristics and theoretical molecular backscatter coefficients of the air and the water near ocean surface.

Using Eq. 4, beam attenuation (red line in Fig. 7) was computed from the HSRL ocean surface depolarization ratio (blue line in Fig. 7) and diffuse attenuation coefficient (black line). The beam attenuation coefficients compare reasonably well with the in-water measurements (green line in Fig. 7). However, the in-water measurements were made several days after the aircraft measurements, as a frontal system moved through the region just after the July 26 flight. This time offset might be partially responsible for the differences between two measurements.

5. CONCLUSIONS

This study introduces an approach for estimating the beam attenuation coefficient, *C,* from lidar depolarization measurements and ocean color- or lidar-based diffuse attenuation coefficients. The concept is based on a theoretical formula established from Monte Carlo simulations that links depolarization ratio of sea water to the multiple scattering factor (the ratio of diffuse attenuation and *c*). The lidar-based *C* retrievals compare reasonably well with ocean color based estimates and in-water measurements.

In the future, the improved HSRL measurements at both 355nm and 532nm could further improve the accuracy of diffuse attenuation coefficient retrievals. Furthermore, CDOM absorption could be estimated from the dual wavelength K_d measurements [14], while dual wavelength backscatter and extinction retrievals could provide information on particle size distributions [15] and composition. By extending these developments to a space-based lidar, significant advances could be realized in quantifying ocean carbon cycle processes.

ACKNOWLEDGEMENT

The authors would like to thank the CNES mission operations team for enabling the 30° pitch maneuver and Drs. Paula Bontempi, Hal Maring and David Considine of NASA CALIPSO, ACE, and SABOR projects and NASA radiation science program for supporting this study.

REFERENCES

[1] Hu, Y., et al., 2008: "Sea surface wind speed estimation from space-based lidar measurements", Atmos. Chem. Phys., **8**, 3593-3601.

[2] Behrenfeld, M.J., et al. (2013), Space-based lidar measurements of global ocean carbon stocks, Geophys. Res. Lett., **40**, doi:10.1002/grl.50816.

[3] Lu, X., et al. (2014), Ocean subsurface studies with the CALIPSO spaceborne lidar, J.G.R., **119**, 4305–4317, doi:10.1002/2014JC009970.

[6] Behrenfeld, M. and E. Boss (2006), Beam attenuation and chlorophyll concentration as alternative optical indices of phytoplankton biomass. J. Mar. Res . **64**, 431-451.

[4] Boss, E. et al., (2009), Acceptance angle effects on the 42 beam attenuation in the ocean. Optics Express **17**(3); 1535-1550.

[5] Voss, K.J (1992), A spectral model of the beam attenuation coefficient in the ocean and coastal areas, Limn. and Ocean., 37, doi: 10.4319/lo.1992.37.3.0501.

[7] Churnside, J. (2014), Review of profiling oceanographic lidar, Optical Engineering, 53(5) 051405 doi: 10.1117/1.OE.53.5.051405.

[8] Hu, Y. et al. (2006), A simple relation between lidar multiple scattering and depolarization for water clouds, Optics Letters, **31**, 1809-1811.

[9] Hu, Y. (2007), Depolarization ratio–effective lidar ratio relation: Theoretical basis for space lidar cloud phase discrimination, Geophys. Res. Lett., **34**, L11812, doi:10.1029/ 2007GL029584.

[10] Hu, Y. et al. (2007), The depolarization-attenuated backscatter relation: CALIPSO lidar measurements vs. theory, Opt. Exp., **15**, 5327–5332.

[11] Gordon, H.R. (1989), Theoretical aspects of hydrologic optics, Limnol. Oceanogr., 34, 1389-1409.

[12] Hair, J.W., et al. (2008), Airborne High Spectral Resolution Lidar for profiling aerosol optical properties, Appl. Opt., **47**, 6734-6752

[13] Hostetler, C.A et al. (2014), Applications of lidar systems for ocean ecosystem and ocean-atmosphere studies, Oc. Opt. XXII, Portland, ME, 26-31 October.

[14] Mannino, A. et al. (2013), Algorithm development and validation of CDOM properties for estuarine and continental shelf waters along the northeastern U.S. coast, Rem. Sens. of Env., **152**, 576-602.

[15] Kostadinov, T. S., et al. (2009), "Retrieval of the particle size distribution from satellite ocean color observations." JGR: Oceans (1978–2012) 114.C9.